Int. J Multiphase Flow Vol 12, No 4, pp 641–653, 1986
Printed in Great Britain

0301-9322/86 $3.00 + .00
Pergamon Journals/Elsevier

STEAM–WATER VOID FRACTION FOR VERTICAL UPFLOW IN A 73.9 mm PIPE

D. R. H. BEATTIE†
Australian Atomic Energy Commission, Private Mail Bag, Sutherland, 2232, Australia

and

S. SUGAWARA
Power Reactor and Nuclear Fuel Development Corporation, 4002 Narita, O-arai, Ibaraki, Japan

(*Received* 6 *February* 1985; *in revised form* 26 *August* 1985)

Abstract—Forced flow and natural circulation void fraction data are presented for steam–water upflow in a 73.9 mm pipe. Nondevelopment apparent in some of the data is due to bubble retardation at a nearby upstream bend. Through the use of suitable approximations, a previous analysis of distributed and annular flow voidage has provided a simple but accurate predictive method for the "developed flow" component of the data.

1. INTRODUCTION

Prediction of cross-section averaged void fraction $\langle\alpha\rangle$ is important for many industrial applications of two-phase flow. In the special case of nuclear reactor technology, predictive methods need to be valid for steam–water flows in moderately sized ducts at high and low pressure; high and low mass flux; and high and low voidage. Due to limitations on available steam–water void data, validation of current predictive methods is not yet possible for all the above conditions. Available data, such as that of Colombo *et al.* (1967) and Hughes (1958), only extend to high voidage and high velocity conditions in comparatively small ducts. Conversely, larger duct data is limited to low voidage, low velocity conditions.

The Japanese boiling light water cooled, heavy water moderated, pressure tube type Advanced Thermal Reactor (ATR), currently under development by the Power Reactor and Nuclear Fuel Development Corporation (PNC), uses 73.9 mm pipework. In order to obtain data relevant to both normal and abnormal ATR operation, and to develop suitable predictive methods for ATR conditions, voidage experiments were performed on such a pipe. The range of flow conditions achieved goes beyond those of other available data. This paper reports these voidage measurements, and describes the prediction method developed from them.

2. DESCRIPTION OF EXPERIMENTS

The voidage experiments were performed on a 14 MW heat transfer loop (HTL) designed to simulate sections of the prototype ATR "Fugen", currently operating in Tsuruga. A flow sheet of the loop is shown in figure 1. In the loop, steam generated at the test section separates from the steam–water mixture in the steam drum, condenses in the high pressure condenser, and returns to the steam drum. The system pressure is adjusted by controlling the heat removal rate from the condenser. This is a vertical shell-and-tube type heat exchanger with the secondary cooling water having a free surface. Thus, system pressure is set by the level of the secondary cooling water. Small adjustments to pressure can be made by venting steam to the atmosphere.

Water separated from the mixture in the drum is cooled in the subcooler, circulated by the pump at a predetermined flow rate, heated by a 1.2 MW capacity preheater to control subcooling, and then enters the heated test section. This test section, as shown in figure 1, is used for rod bundle critical heat flux and similar experiments. The present data

† Work performed while attached to the Power Reactor and Nuclear Fuel Development Corporation.

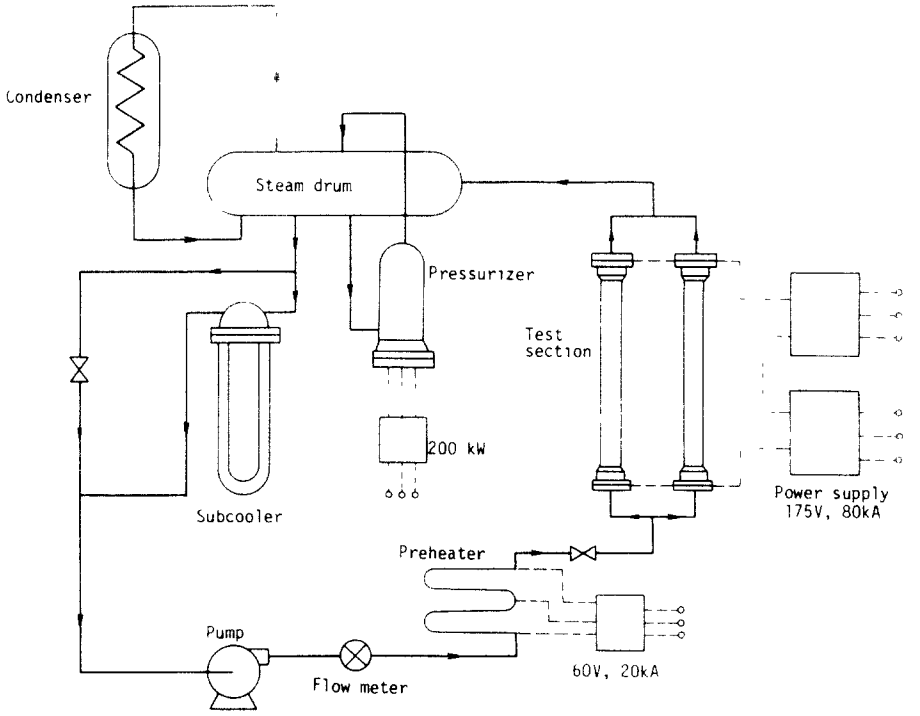

Figure 1 Flow sheet of heat transfer loop (HTL)

were not obtained here but were instead obtained in a vertical adiabatic 73.9 mm section of the pipework downstream of the test section. Mixture and gas superficial velocities $\langle j \rangle$ and $\langle u_G \alpha \rangle$ in this section were not measured directly but instead calculated from the measured mass flow and the quality x obtained from a heat balance, i.e. from

$$\langle j \rangle = \frac{G}{\rho_L} \left\{ 1 + x\left(\frac{\rho_L}{\rho_G} - 1\right) \right\}$$

and

$$\langle u_G \alpha \rangle = \frac{Gx}{\rho_G}$$

where G is the mass flux and ρ_L, ρ_G are liquid and gas densities.

A γ-ray void meter, using a 2 Ci Cs-137 gamma source collimated into a 5 mm diameter beam, was used for the voidage measurements. Most data were obtained with "one-shot" measurements at the tube centre line; however, complete scans were made at several conditions in order to construct a calibration curve for converting the one-shot data into mean void fraction values. Details are given by Obata *et al.* (1975).

As shown in figure 2, data were obtained at 8.5 and 25 diameters (63 and 185 cm) downstream of a 90° bend. At both positions, forced circulation experiments were performed at 7 MPa. These had mass fluxes of 640, 1280, 1900, and 2600 kg m^{-2} s^{-1}. Natural circulation experiments were also performed at the position 8.5 diameters from the bend at pressures of 0.2, 1, 3, and 7 MPa. These had mass fluxes ranging from 51 to 300 kg m^{-2} s^{-1}.

Voidage errors were estimated to be about $\pm 2.5\%$, being due to $\pm 0.5\%$ from the γ-attenuation, allowing for pipe thickness, together with $\pm 2\%$ from the detector instrumentation. This is consistent with errors of other researchers, as summarized by Jones (1981), and is compatible with the degree of nonrepeatability observed in the experiments. Errors in mass flux, measured with a turbine meter or differential pressure device, were about $\pm 2\%$, and errors in steam quality were about $\pm 5\%$, being due to errors in mass flux, power

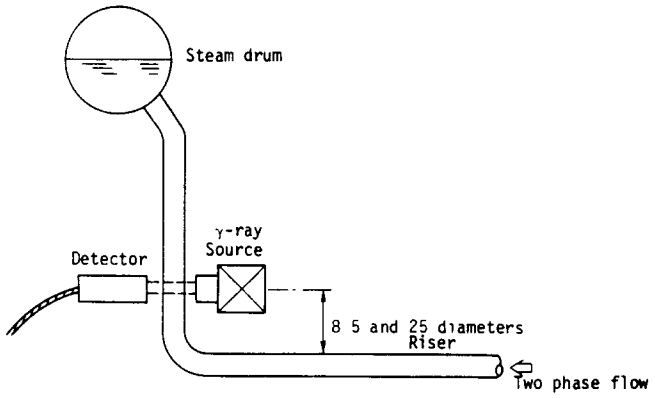

Figure 2. Position of γ-ray void meter.

(±1.5%), pressure (±0.5%) and temperature (±0.3%). Data at the downstream position were obtained at an earlier date. Errors for these data are slightly greater than those quoted above.

3. THEORETICAL BACKGROUND

The experimental data are later interpreted in terms of theoretical concepts (Beattie 1976, 1977) developed for distributed (e.g. bubble, slug) and separated (e.g. annular) two-phase flows. In the present application of the theory, various approximations are included in order to simplify the predictive method resulting from the analysis. These remove the need for iterative calculation procedures, and allow predictions of a comparable accuracy to those of the original method to be made at pocket calculator level.

3.1 Distributed flows

The drift-flux equation

$$\frac{\langle u_G \alpha \rangle}{\langle \alpha \rangle} = C_0 \langle j \rangle + V, \qquad [1]$$

developed by Zuber and his co-workers (Zuber *et al.* 1967; Zuber & Findlay 1965) in their extension of a generalization of earlier work, is used as a basis for the present analysis. In [1], V is a drift velocity which allows for local "slip" effects, and C_0 is a "distribution parameter" which accounts for phase and velocity distribution effects.

As discussed by Zuber *et al.*, the drift velocity for developed vertical slug flow is

$$V = 0.35 \sqrt{g D \Delta\rho/\rho_L}, \qquad [2]$$

where g is the gravitational acceleration, D is the tube diameter, and $\Delta\rho$ is $\rho_L - \rho_G$. For developed bubble flow, the drift velocity recommended by Zuber *et al.* is

$$V = 1.4 \left(\sigma g \frac{\Delta\rho}{\rho_L^2}\right)^{0.25}, \qquad [3]$$

where σ is the surface tension.

Although the distribution parameter C_0 of [1] is normally determined empirically, it has been shown (Beattie 1976) that it can often be identified with the maximum-to-average velocity ratio $j_m/\langle j \rangle$. For a two-phase version of the "universal" velocity profile, this led to a predictive equation for the distribution parameter C_0 given by

$$C_0 = 1 + 2.6 \sqrt{f}, \qquad [4]$$

where f is the Fanning friction factor obtained from

$$\frac{1}{\sqrt{f}} = 4 \log \mathrm{Re} \sqrt{f} - 0.4 , \qquad [5]$$

with Re being the Reynolds number appropriate for a bubbly viscous sublayer:

$$\mathrm{Re} = \frac{D G}{[\mu_L(1 + 2.5 \beta)]} . \qquad [6]$$

In this definition, G is the total mass flux, μ_L is the liquid viscosity, and β is the overall gas volume flow fraction.

Distributed flow voidage for developed upflow is thus predicted from [1], [2] or [3], and [4]–[6]. Although straightforward, the method is simplified here by replacing [5] with an explicit friction factor equation

$$f = 5.525 \times 10^{-2} \mathrm{Re}^{-0.2370} + 8.0 \times 10^{-4} , \qquad [5a]$$

which closely approximates [5] over conditions of interest, and [6] with

$$\mathrm{Re} = \frac{D G}{3 \mu_L} . \qquad [6a]$$

Clearly, these simplifications introduced into the C_0 calculation method will be more accurate at higher gas volume flow ratios. However, errors introduced at lower voidages will be small since [4] and [5] (or [5a]) point to only a small influence of Reynolds number on C_0. In addition to this, there are two features of [1]–[6] which indicate that errors introduced into calculated void fractions by introducing approximations [5a] and [6a] will not only be small, but will be very small:

(a) Low voidage high velocity data necessarily have high Reynolds numbers as defined by [6]. Since friction factors vary only slightly with Reynolds number under such conditions, approximation [6a] will have only a very small influence on C_0 as calculated by [4];

(b) Conversely, lower velocity low voidage flows will have distribution parameters which vary more with void fraction, so approximation [6a] is not as good. However, under these conditions, the void fraction is influenced more by the drift velocity than by the distribution parameter. (Moreover, errors in calculated value of C_0 still remain small.)

In addition to these points, we note that errors introduced into calculated values of low void fractions translate into smaller fractional errors in the more important values of liquid volume fraction.

3.2 Annular flows

Although [1] has been used elsewhere as a basis for annular flow void fraction correlation, for example by Zuber *et al.* (1967), the distributed nature of the drift-flux model behind [1] is inappropriate for annular flows. Moreover, apparently good correlations of high voidage values of $\langle u_G \alpha \rangle / \langle \alpha \rangle$ may in fact contain significant errors when viewed in terms of the more important liquid volume fraction. Consequently, we have chosen to consider instead an annular flow liquid volume fraction equation obtained from the relation between the liquid film thickness $s = (1 - A)D/4$, where A is the core volume fraction, and the film volume flow Q_f. This relation is derived by integrating the velocity profile over the film region:

$$Q_f = \int_0^s j \pi D \, dy , \qquad [7]$$

where y is the distance from the wall.

The particular version of thin-film approximation used in [7] has been examined and found to be remarkably accurate for all film thicknesses.

Equation [7] leads to a relation between film volume flow ratio $1 - B = Q_f/(Q_f + Q_c)$, where subscripts f and c refer to the film and core, and the film volume fraction $1 - A$. Introducing core region and film region void fractions and volume flow fractions α_f, α_c, β_f, β_c to allow for film bubbles and core droplets, then

$$1 - A = \frac{(\alpha_c - \langle\alpha\rangle)}{(\alpha_c - \alpha_f)}, \qquad [8a]$$

$$1 - B = \frac{(\beta_c - \beta)}{(\beta_c - \beta_f)}. \qquad [8b]$$

Thus, [7] becomes a relationship between void fraction and volume flow fraction if the regional void parameters α_f, α_c, β_f, β_c are specified.

In a previous analysis (Beattie 1977), [7] was developed using a two-phase version of the "universal" velocity profile. Unfortunately, this led to an implicit, rather than explicit, relation for void fraction. In the present analysis, an explicit relation is achieved by using instead a $1/n$ power relationship for velocity; i.e. $j \sim y^{1/n}$. This leads to the simple relation†

$$(1 - A) = (1 - B)^{n/(n+1)}. \qquad [9]$$

Further simplification is achieved by neglecting core droplets, i.e. by assuming $\alpha_c = \beta_c = 1$, and by assuming that, for a given mass flux, the film regional void parameters α_f and β_f do not vary with overall void fraction. Continuity of the predicted void characteristics at the annular flow regime boundary can be ensured by choosing for α_f and β_f the average void fraction and volume flow fraction at the transition:

$$\alpha_f = \langle\alpha_{TR}\rangle, \quad \beta_f = \beta_{TR},$$

where the subscript TR refers to the regime transition value. Clearly, from [1], $\langle\alpha_{TR}\rangle$ and β_{TR} are related by

$$\langle\alpha_{TR}\rangle = \frac{\beta_{TR}}{(C_0 + V/\langle j_{TR}\rangle)}.$$

A sensitivity study has shown that the above assumptions are reasonable at lower voidage annular flows, and tend to compensate each other at higher voidage annular flows. However, the neglect of core droplets becomes unacceptable at very high void fractions as the dry-wall droplet flow regime is approached.

A value of n for the $1/n$ power law is required to complete the analysis. The value should provide a power law velocity profile which approximates the "universal" form. We ensure that the approximation is reasonable by choosing n so that $j_m/\langle j\rangle$ is the same for both profiles. For a $1/n$ power law $j_m/\langle j\rangle = (n + 1)(2n + 1)/(2n^2)$. This is equated to C_0 to find n. The value of n so obtained varies with Reynolds number and ranges from 6.6 to 10.5 for the present data.

Collecting the various steps and assumptions, the relationship for annular flow void fraction becomes

$$1 - \langle\alpha\rangle = (1 - \langle\alpha_{TR}\rangle)\left(\frac{1 - \beta}{1 - \beta_{TR}}\right)^{2/(-1 + \sqrt{8C_0 + 1})}, \qquad [10]$$

where C_0 is calculated from [4].

† Actually, because of the thin-film approximation, a near unity constant appears in the rhs of [9]. This is made equal to unity to ensure validity at the zero-core limit of annular flow.

As described in section 4, a regime transition criterion appropriate to the present data has been obtained empirically from the data. This removes the unknowns $\langle \alpha_{TR} \rangle$ and β_{TR} from the rhs of [10] and permits [10] to be used for predictive purposes

3.3 Some considerations on flow nondevelopment

As discussed in more detail in section 4, void characteristics differed at the two axial measurement locations. In view of the close proximity of the upstream location to an upstream pipe bend (see figure 2), it is possible that the void differences may be due to flow being less developed at this position (For the purposes of this paper, "developed flow" is used here to indicate an absence of upstream effects an average void fraction).

Some insight into upstream effects on average void fraction was gained by Beattie & Lawther (1981) from their void data for seven-rod clusters. Some of their data are shown in figure 3. Their slug flow data behave in a "developed" manner, and are consistent with the analysis of section 3.1, provided the round tube slug drift velocity expression [2] is modified for rod bundles as described by Griffith (1964). On the other hand, their bubble flow data provided distribution parameters which were considerably larger than those normally encountered and, unexpectedly for upflow, negative drift velocity values close in magnitude to the superficial liquid velocity. They related their negative drift velocities to observations of gas "wakes" on the spacers used to separate the rods, and hypothesized that bubbles in the flow are entrained into the wakes. On leaving the wakes, gas bubbles enter the flow with an initial zero velocity with respect to the spacers, i e. with a negative drift with respect to the flow

A simplified analysis is given here which assumes that a similar bubble retardation mechanism occurred at the bend upstream of the present experiments. The analysis considers a single bubble, with zero initial velocity and terminal drift velocity given by [3], in an

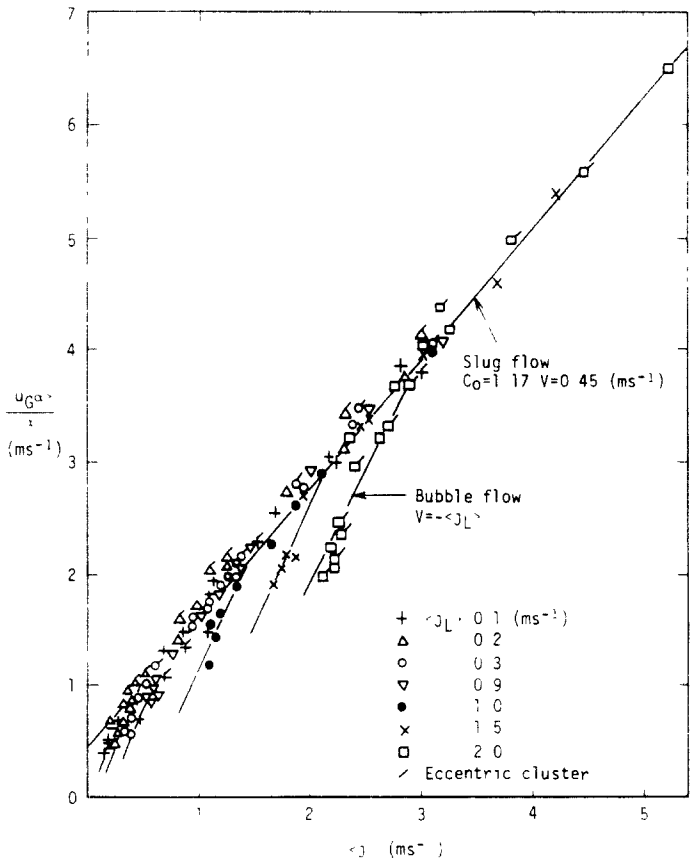

Figure 3 Nondevelopment in bubble flow average voidage data for bowed and nonbowed 42 mm equivalent diameter rod clusters Adapted from Beattie & Lawther (1981)

infinite liquid upflow of velocity $\langle j \rangle$. The velocity development of this bubble is assumed to be similar to that occurring downstream of the bend of our experiment. The analysis estimates the distance required for the terminal drift velocity to be attained. As this distance varies with $\langle j \rangle$, estimates can be obtained of the maximum velocities beyond which flow will be undeveloped at the void measurement locations. Thus void fraction development is considered only in terms of the drift velocity, but not in terms of the distribution parameter, which may also be effected by the bend. However, data analyses, such as that presented by Zuber *et al.* (1967), suggest that void fractions for flows which have achieved the terminal drift velocity also have a "developed"distribution parameter. (We point out that several of the data examined by Zuber *et al.* demonstrate a negative drift of the type discussed here. However, they apparently interpreted these data instead in terms of a developed, terminal drift velocity, and a strongly varying, developing distribution parameter.)

We start with the equation of motion for a bubble in vertical upflow:

$$\Delta\rho\, g \pm K\rho_L \frac{(v - \langle j \rangle)^2}{d} = \frac{\mathrm{d}}{\mathrm{d}t}(\rho_G + \rho_L)(v - \langle j \rangle)\,. \qquad [11]$$

In the above, K is the bubble drag coefficient, assumed invariant over the development length; d is the bubble diameter; and v is the bubble velocity. The three terms represent the forces due to gravity, drag, and acceleration.

The drag term is positive for $v < \langle j \rangle$ when drag assists buoyancy, and negative for $v > \langle j \rangle$. In view of the known steady-state drift velocity given by [3], $K\rho_L/(\Delta\rho g d)$ can be replaced by $1/V^2$.

The "added mass" component of the acceleration term, $\mathrm{d}\rho_L(v - \langle j \rangle)/\mathrm{d}t$, represents acceleration of the liquid surrounding the bubble. Some liquid is accelerated with the bubble because nearby liquid is constrained to move with the bubble. The added mass term has a coefficient 0.5 in creeping flow; we have used a unity coefficient as this is representative of values found by Odar & Hamilton (1964) in their higher Reynolds number experiments.

Equation [11] may be integrated to show that the bubble will be within 10% of its terminal drift velocity after traveling a distance s given by

$$s = \frac{V(\rho_G + \rho_L)\langle j \rangle}{g\,\Delta\rho}\left\{1.47 + \tan^{-1}\frac{\langle j \rangle}{V} + \frac{V}{\langle j \rangle}\left(1.52 + \log\frac{V}{(V^2 + \langle j \rangle^2)^{1/2}}\right)\right\}. \qquad [12]$$

From this estimate of flow development length, bubble flows will not be developed at the upstream void measuring position for velocities greater than 11.7 m s^{-1}, and will not be developed at the downstream position for velocities greater than 31.5 m s^{-1}. (These figures refer to 7 MPa; slight differences occur at other pressures).

The above analysis is for bubble flows. Developing slug flows are more complex since they involve a nonslugging region of coalescing bubbles. However, the bubble retarding mechanism proposed here means that the coalescing bubble region will be smaller than for bubbles flowing at their terminal velocity, so this region may be neglected. Errors so introduced are to some extent compensated by neglect of the interaction between developing slugs. This can produce high drift velocities in developing slug flow (Moissis & Griffith 1962). Thus, the above bubble flow analysis may reasonably be applied to slug flow by replacing the terminal drift velocity with that for slug flows, [2]. This yields critical flow velocities above which slug flows are unlikely to be developed at the upstream and downstream measurement locations of 6.5 and 18.5 m s^{-1}, respectively.

The annular flow model presented in section 3.2 is one with entrained film bubbles. Since annular flows considered here are of comparatively low voidage and the films are assumed to contain entrained bubbles, the films should be comparatively thick. This means that the bubble retardation mechanism proposed for bubble flows can plausibly be extended to entrained film bubbles in annular flows. Consequently, critical flow velocities for developed annular flows should be close to those calculated above for bubble flows.

The above, together with estimates of flow regime transitions for the present range of flow conditions suggest that, to a first approximation, the natural circulation flows can be

expected to be developed at both measurement positions, but the forced circulation flows will be developed only at the downstream position.

Although this will be examined in more detail later, we note here that the above conclusion is qualitatively consistent with the different forced-convective void characteristics for the two measurement positions.

4 DATA ANALYSIS

4.1 Analysis in the drift-flux plane

Figures 4–6 present the data in terms of parameters suggested by the drift-flux model. mean gas velocity $\langle \alpha u_G \rangle / \langle \alpha \rangle$ as a function of mean mixture velocity $\langle j \rangle$. Although each figure demonstrates special features of the data, which are discussed below, it can be seen from the figures that in all cases the drift-flux interpretation provides reasonable correlation of the data.

The distribution parameter (1.09) and drift velocity (0.8 m s^{-1}) for the lowest pressure natural circulation data (figure 4) differ considerably from those predicted from the distributed flow theory of section 3.1. They are, however, typical of those encountered for annular flow (Zuber *et al.* 1967). These data can therefore be associated with the annular flow regime; a conclusion which is confirmed below is the analysis of section 4.2.

Figure 5 compares bubble and slug flow predictions with the higher pressure natural circulation data. (Actually, predicted distribution parameters are about 1.185 for the 3 MPa data and range from 1.205 to 1.27 for the 7 MPa data. The variation cannot be adequately represented graphically, so the "predicted" curves of figure 5 have been drawn with a representative distribution parameter of 1.2). This figure confirms the "developed" condition predicted for these data, and also confirms the predicted developed flow characteristics.

It is apparent that some data scatter in figure 5 can be explained in terms of regime change effects. An attempt was made to obtain the bubble/slug flow regime boundary from this plot. However, due to an insufficient range of flow conditions, an adequate estimate of this boundary could not be achieved.

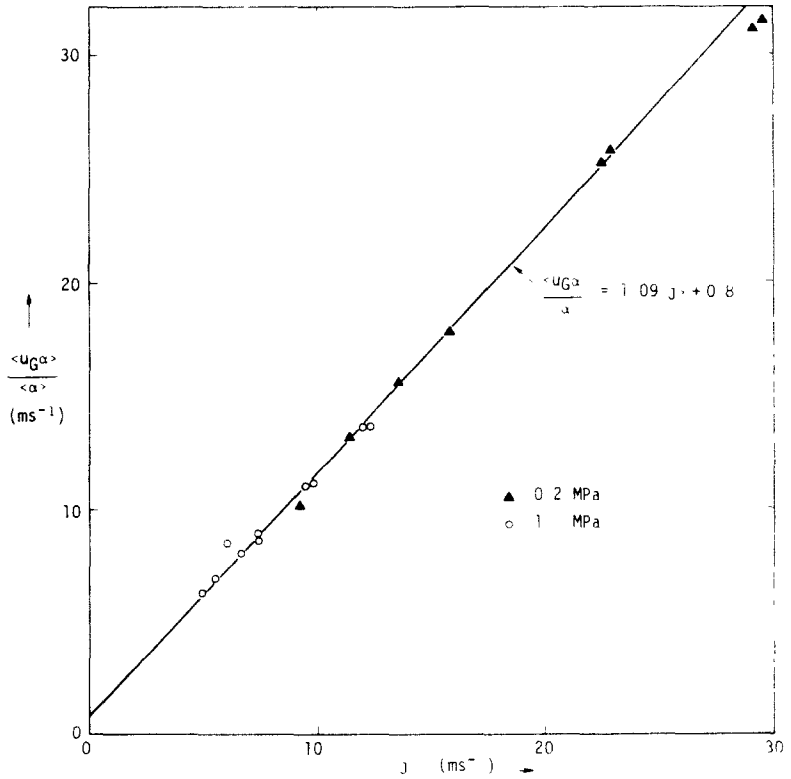

Figure 4 Natural circulation void data at 0.2 and 1 MPa

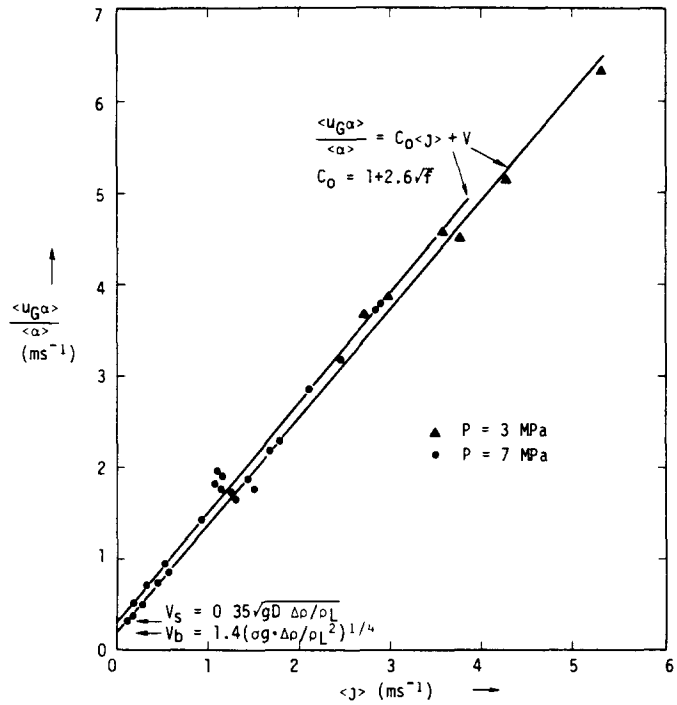

Figure 5. Natural circulation void data at 3 and 7 MPa.

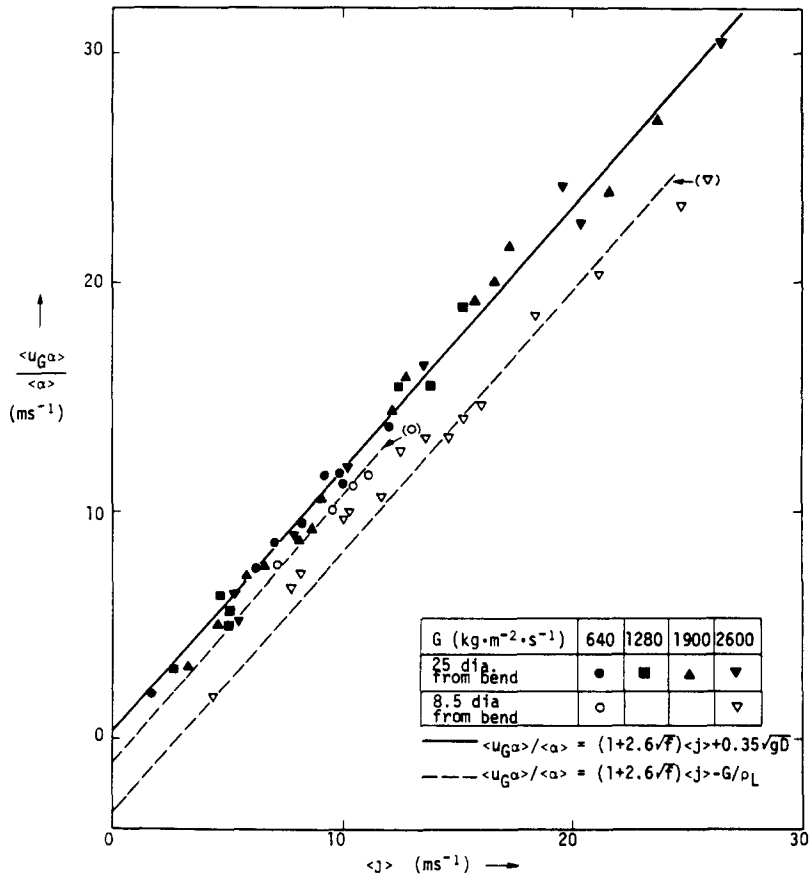

Figure 6. Forced circulation void data at 7 MPa.

The 7 MPa forced-convection void data are shown in figure 6. For clarity, the upstream data at 1280 and 1900 kg m^{-2} s^{-1} have been omitted from the graph; these behave in a similar manner to the upstream 640 and 2600 kg m^{-2} s^{-1} data. Again, a single representative predicted distribution parameter 1.155 has been used in the predicted curve for the downstream data, although actual predictions vary from 1.147 at the highest mass flux to 1.167 at the lowest mass flux.

As expected from the analysis of section 3.3, the downstream data are close to the "developed" flow predictions of section 3.1, although some evidence of residual nondevelopment is apparent. In contrast to these results, the data of Sekoguchi (1969) indicate the horizontal flow development is not achieved as rapidly. On the other hand, the upstream data, although reasonably represented with the developed flow distribution parameter, have a negative drift velocity of magnitude approximately G/ρ_L. This is qualitatively consistent with nondevelopment predicted for these data in section 3.3.

The high velocities in the data of figure 6, together with the data scatter, meant that, unlike the data of figure 5, the plot could not be used to determine which downstream data had a bubble drift velocity and which had a slug drift velocity. The "predicted" curve is the prediction for slug flow.

4.2 Presentation in the $1-\langle\alpha\rangle:1-\beta$ *plane*

The natural circulation data and the downstream forced circulation data, being for developed flow conditions, are presented in figure 7 in terms of the liquid volume fraction as a function of liquid volume flow fraction. As noted, the liquid volume fraction is of more interest than the void fraction parameter $\langle u_G \alpha\rangle/\langle\alpha\rangle$ high lighted by the drift-flux model. Since the liquid volume fraction can vary considerably with mass flux, data obtained at more arbitrary mass fluxes have been omitted from the graph.

Also shown are predictions from section 3. These use a slug flow drift velocity at lower voidages and an annular flow regime boundary given by $\langle\alpha_{TR}\rangle = 0.80$. The slug flow drift velocity was chosen in the absence of a verifiable bubble-slug regime transition criterion for the system under study, even though, clearly (for example see figure 5) some data are for bubble flows. For the lower void lower velocity bubble flows, the assumption may lead to large errors in predicted voidage. However, this translates to comparatively small errors in predicted liquid volume fraction.

The annular flow regime transition criterion $\langle\alpha_{TR}\rangle = 0.80$ was chosen empirically on the basis of applicability ranges of the distributed and annular models of section 3. We note that the annular flow interpretation of the low pressure natural circulation data obtained from figure 4 is confirmed in figure 7. On the other hand, figure 7 also indicates that some

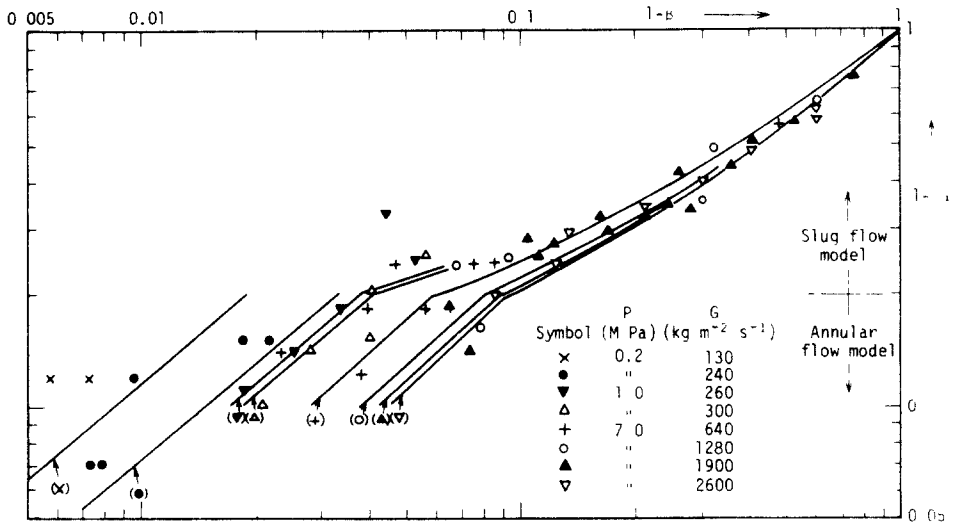

Figure 7 Comparison of liquid volume fraction data with theory

forced circulation data are also for annular flow. This is not apparent from the drift-flux analysis of these data in figure 6. Note however that, since annular flow void characteristics differ from those for nonannular flows, the inclusion of annular flow data contributes to data scatter in figure 6.

5. DISCUSSION

Figure 7 indicates that the theory of sections 3.1 and 3.2, which is a simplified version of an earlier analysis, adequately describes the present developed flow liquid volume fraction data, even with the slug flow prediction also being applied to bubble flows. The one empirically determined component of the predictive method, an annular flow regime boundary given by $\langle \alpha_{TR} \rangle = 0.80$, is particularly simple in form. Thus, the present work leads to a simple predictive method for developed steam-water void fractions in ATR vertical riser tubes. Since, apparently, flow development is reestablished rapidly after disturbances, errors introduced by applying the method to nondeveloped regions will be small.

The annular flow component of the present data are consistent with the assumption that the film region void fraction and volume flow ratio do not vary with overall void fraction. For the present data, the film voidage $\alpha_f \equiv \langle \alpha_{TR} \rangle$ has been estimated to be 0.8. The corresponding film volume flow ratio $\beta_f \equiv \langle \beta_{TR} \rangle$ varies with mass flux [see point (2) below], and, from figure 7, ranges from 0.91 to 0.98 for the present data.

Collecting the various steps of the analysis, the predictive method can be summarized as:

(1) For a given flow, calculate the distribution parameter from

$$f = 5.525 \times 10^{-2} \left[\frac{D\,G}{(3\,\mu_L)} \right]^{-0.237} + 8.0 \times 10^{-4},$$

$$C_0 = 1 + 2.6\sqrt{f}.$$

(2) Calculate the gas volume flow fraction β_{TR} corresponding to an annular flow regime transition given by $\langle \alpha_{TR} \rangle = 0.80$;

$$\beta_{TR} = 1 - \frac{1 - 0.80\,(C_0 + \rho_G\, V_s/G)}{1 + 0.80\,(\rho_L - \rho_G)\, V_s/G},$$

where $V_s = 0.35\, g\, D\, \Delta\rho/\rho_L$.

(3) For $\beta \leq \beta_{TR}$,

$$\langle \alpha \rangle = \frac{\langle \alpha u_G \rangle}{C_0 \langle j \rangle + 0.35 \sqrt{g\, D\, \Delta\rho/\rho_L}}.$$

(4) For $\beta > \beta_{TR}$,

$$(1 - \langle \alpha \rangle) = 0.20 \left(\frac{1 - \beta}{1 - \beta_{TR}} \right)^{2/(-1 + \sqrt{8C_0 + 1})}.$$

The method could be improved by allowing for

- a more accurate drift velocity representation; in particular, the separation of distributed flows into the bubble and slug regimes, together with a method for predicting the boundary between these regimes;
- an improved annular flow transition criterion;
- nondevelopment of voidage following flow disturbances;
- core droplets in annular flow.

The theory of section 3 could be used to assist in the development of some of these improvements. However, any such improvements would be at the expense of the simplicity

achieved with the present method. In any case, predictions from the present method appear adequate despite the assumptions involved; the method predicts the data of figure 7 to an accuracy comparable to the data scatter.

The present experiments cover a comparatively limited range of conditions, although they do go beyond the ranges covered by other available data. The agreement of the theory with the data has been achieved with very little introduced empiricism, suggesting that its applicability may be extended beyond the present range of conditions. We note that the original but more complex version of the present analysis appears to be valid for a considerable range of void data (see e.g. Beattie 1976, 1977, 1979; Beattie & Lawther 1981). However, the data analysis in these works suggests that there are two aspects of the theory which are not general, so caution should be applied when extending the predictive method to other flow conditions.

The first of these concerns mean flow structure. The present analysis assumes a "universal" type velocity profile with a bubbly sublayer for low voidage flows. Pressure loss analyses (Beattie 1977) show that while this is generally true exceptions occur. The theory then remains valid, provided a different form of nondimensional velocity profile is used. Related to this, flow stratification may occur in horizontal flows, particularly for larger ducts. Clearly, the present analysis will be inappropriate for a sufficient degree of stratification. (Of course, nonstratified horizontal flows require a zero drift velocity for the prediction method.)

The second point concerns the annular flow regime criterion, determined here to be $\langle\alpha_{TR}\rangle = 0.80$. Being empirical, it's general validity must be doubted. In this regard, an earlier but similar study on steam–water void fraction (Beattie 1979) empirically determined a criterion which was similar in form but smaller in magnitude, $\langle\alpha_{TR}\rangle = 0.55$. The earlier criterion is consistent with several high pressure visually-based regime maps (Bartolemei & Georgescu 1966; Bennett *et al.* 1965; Alia *et al.* 1965). However, ducts for the earlier voidage analysis and for the regime maps were smaller than that considered here. Recent regime transition studies, such as that of Crawford & Weisman (1984), show that regime boundaries are influenced by channel equivalent diameter.

The effect of duct size on another parameter of the theory, the distribution parameter, is predictable from the theory. Because of the large Reynolds numbers in the present forced-convection data, predicted distribution parameters ($\sim$1.15) are smaller than for the other steam–water data (Zuber *et al.* 1967). On the other hand, the present natural circulation data have Reynolds numbers similar to those of other studies, and consequently have similar distribution parameters.

We close this discussion by quantifying a comparative aspect of the two different method of data analysis used here. We have said that the drift-flux interpretation may camouflage errors at high voidages. This is because high void data must necessarily approach $\langle\alpha u_G\rangle/\langle\alpha\rangle = \langle j\rangle$. To demonstrate the point, we consider the two highest velocity data of figure 4 These correspond to the two lowest 1-β data of figure 7. Although the figure 4 correlation appears to describe these data better than the correlation of figure 7, the figure 4 correlation errors for $1 - \langle\alpha\rangle$ are in fact about twice those for figure 7.

6 SUMMARY AND CONCLUSIONS

As part of the developmental program for the Japanese Advanced Thermal Reactor project, void fractions have been measured in a vertical 73.9 mm pipe for steam–water flowing in both forced and natural circulation conditions. The data show evidence of being affected by a nearby upstream bend. The extent of nondevelopment is qualitatively consistent with a theoretical analysis of flow disturbance effects on bubble drift velocities. The analysis indicates that void development following a flow disturbance is reestablished rapidly.

A modified version of a previous theoretical analysis of distributed and annular flow void fractions has led to a simple and accurate predictive method, summarized in section 5, for the flows considered here. In the method, preannular flows are treated as slug flows. The treatment for annular flows allows for film bubbles but not core droplets. Apart from a simple criterion for the annular flow boundary, the method involves no introduced empiricism.

Acknowledgement—The contribution of one of us (D.R.H.B.) was made possible through an award provided by the Japan Science and Technology Agency.

REFERENCES

ALIA, P., CRAVAROLO, L., HASSID, A. & PEDROCCHI, E. 1965 Liquid volume fraction in adiabatic two-phase vertical upflow-round conduit. CISE-R-105.

BARTOLEMEI, G. G. & GEORGESCU, R. 1966 Experimental study of the hydrodynamics of two-phase flow in vertical pipes. IFA (Bucharest) report TR-52; UKAEA Report AERE Trans. 1076.

BEATTIE, D. R. H. 1976 Pressure pulse and critical flow behaviour in distributed gas/liquid systems. *Proc. 2nd Int. Conf. Pressure Surges*, London, U.K.

BEATTIE, D. R. H. 1977 Some aspects of two-phase flow drag reduction. Proc. 2nd Int. Conf. Drag Reduction, Cambridge, U.K.

BEATTIE, D. R. H. 1979 Two-phase pressure loss and void fraction characteristics in rod bundle geometries. *Proc. XVIII IAHR Congress*, Cagliari, Italy.

BEATTIE, D. R. H. & LAWTHER, K. R. 1981 Two-phase hydrodynamic experiments with axial flow through seven-rod clusters. *Int. J. Multiphase Flow* **7**, 423–437.

BENNETT, A. W., HEWITT, G. F., KEASSEY, H. A., KEEYS, R. K. F. & LACEY, P. M. C. 1965–66 Flow visualization studies of boiling at high pressure. UKAEA Report AERE-R-4874.

COLOMBO, A., ERA, A., HASSID, A., PREMOLI, A., SPADONI, B. & ZAVATTARELLI, R. 1967 Density measurements with two-phase mixtures in adiabatic and heated channels at high pressure by means of a quick closing valve method. Centro Informazioni Studi Esperienze (Milano) Report CISE-R-225.

CRAWFORD, T. & WEISMAN, J. 1984 Two-phase (vapor–liquid) flow pattern transitions in ducts of non-circular cross-section and under diabatic conditions. *Int. J. Multiphase Flow* **10**, 385–391.

GRIFFITH, P. 1964 The prediction of low quality voids. *J. Heat Transfer* **86**, 327–333.

HUGHES, T. A. 1958 Steam–water mixture density studies in a natural circulation high pressure system. Babcock & Wilcox G. Report No. 5435. [Cited in Zuber *et al.* (1967).]

JONES, O. C., Jr. 1981 Experimental methods in two-phase flows. *Articles in Nuclear Reactor Safety Heat Transfer* (Edited by O. C. Jones, Jr.), pp. 857–928. Hemisphere, Washington D.C.

MOISSIS, R. & GRIFFITH, P. 1962 Entrance effects in a two-phase slug flow. *J. Heat Transfer* **84**, 29–39.

ODAR, F. & HAMILTON, W. S. 1964 Forces on a sphere accelerating in a viscous fluid. *J. Fluid Mech.* **18**, 302–314.

OBATA, T., KOBORI, T. & HAYAMIZU, Y. 1975 The development of two-phase flow instrumentation at O-arai Engineering Centre. PNC report N941, pp. 75–84.

SEKOGUCHI, K., SATO, Y. & KARIYASAKI, A. 1969 Influence of mixers, bends and exit sections on horizontal two-phase flow. In *Cocurrent Gas–Liquid Flow*, pp. 109–144. Plenum Press, New York.

ZUBER, N. & FINDLAY, J. A. 1965 Average volumetric concentration in two-phase flow systems. *J. Heat Transfer* **87**, 453–468.

ZUBER, N., STAUB, F. W., BIJWAARD, G. & KROEGER, P. G. 1967 Steady state and transient void fraction in two-phase flow systems. General Electric Report GEAP 5417.